JOURNAL OF MULTIFUNCTIONAL MATERIALS & PHOTOSCIENCE
7(2), December 2016, pp. 71-79

Preparation of $NaGd(MoO_4)_2$:Ho^{3+}/Yb^{3+} Yellow Phosphors via Mcrowave Sol-Gel Route and Upconversion Photoluminescence Properties

Chang Sung Lim*

**Department of Advanced Materials Science & Engineering, Hanseo University, Seosan 356-706, Korea*

Abstact: $NaGd_{1-x}(MoO_4)_2$: Ho^{3+}/Yb^{3+} phosphors with the proper doping concentrations of Ho^{3+} and Yb^{3+} were successfully synthesized by the microwave-modified sol-gel method. Well-crystallized particles formed after heat-treatment at 900°C for 16 h showed a fine and homogeneous morphology with particle sizes of 1-3 μm. The optical properties were examined comparatively using photoluminescence emission and Raman spectroscopy. Under excitation at 980 nm, the upconversion doped samples exhibited strong yellow emissions based on the combination of strong emission bands at 545-nm and 655-nm emission bands in green and red spectral regions, respectively. The strong 545-nm emission band in the green region corresponds to the $^5S_2/^5F_4 \rightarrow {}^5I_8$ transition in Ho^{3+} ions, while the strong emission 655-nm band in the red region appears due to the $^5F_5 \rightarrow {}^5I_8$ transition in Ho^{3+} ions. The spectroscopic properties of the upconversion phosphors were evaluated in detail.

Key words: Upconversion, Double molybdates, Microwave sol-gel, Yellow phosphor

Introduction

Recently, design and synthesis for rare-earth activated photoluminescence particles have attracted considerable attention in their applications, such as fluorescent lamps, cathode ray tubes, solid-state laser, amplifiers for fiber optics communication and new optoelectronic devices, which allow them to overcome many of the current limitations of traditional photoluminescence materials [1-3]. Scheelite-structured compounds belonging to the molybdate family have attracted great attention because of their spectroscopic characteristics and excellent upconversion (UC) photoluminescence properties [4,5]. Most of $NaLn(MoO_4)_2$ (Ln = La^{3+}, Gd^{3+}, Y^{3+}) possess the tetragonal scheelite structure with the space group $I4_{1/a}$, and belong to the family of double molybdates compounds. It is possible for the trivalent rare earth ions in the tetragonal phase to be partially substituted by Ho^{3+} and Yb^{3+} ions. These ions are effectively doped into the crystal lattices of the tetragonal phase due to the similar radii of the trivalent rare earth ions, which results in the excellent UC photoluminescence properties [6-8]. Co-doped Yb^{3+} ion and Ho^{3+} ion can remarkably enhance the UC efficiency for the shift from infrared to visible light due to the efficiency

*Corresponding author: *cslim@hanseo.ac.kr*

of the energy transfer from Yb^{3+} to Ho^{3+}. The Yb^{3+} ion, as a sensitizer, can be dramatically excited by an incident light source energy. This energy is transferred to the activator from which radiation can be emitted. The Ho^{3+} ion activator is the luminescence center of the UC particles, while the sensitizer enhances the UC luminescence efficiency [9-11].

For preparation of the double molybdate $NaLn(MoO_4)_2$, several processes have been developed via specific preparation processes [12-17]. For realized application of UC photoluminescence in products, features such as the homogeneous UC particle size distribution and morphology need to be well defined. Compared with the usual methods, microwave synthesis has advantages of very short reaction time, small-size particles, narrow particle size distribution, and high purity of final polycrystalline samples. Microwave heating is delivered to the material surface by radiant and/or convection heating, which heat energy is transferred to the bulk of the material via conduction [18-20]. It is a cost-effective method that provides high homogeneity and is easy to scale-up, and it is emerging as a viable alternative approach for the quick synthesis of high-quality luminescent materials. However, the $NaGd_{1-x}(MoO_4)_2:Ho^{3+}/Yb^{3+}$ phosphors prepared by the microwave sol-gel method have not been reported.

In this study, $NaGd_{1-x}(MoO_4)_2:Ho^{3+}/Yb^{3+}$ phosphors with the correct doping concentrations of Ho^{3+} and Yb^{3+} (x = Ho^{3+} + Yb^{3+}, Ho^{3+} = 0 and 0.05, and Yb^{3+} = 0, 0.35, 0.40, 0.45 and 0.50) were successfully prepared by the microwave sol-gel method, followed by heat treatment. The synthesized particles were characterized by X-ray diffraction (XRD) and scanning electron microscopy (SEM). Pump power dependence of the UC emission intensity were evaluated in detail. The ospectroscopic properties were examined comparatively using photoluminescence (PL) emission and Raman spectroscopy.

Experimental

In this study, precise amounts of $Na_2MoO_4 \cdot 2H_2O$ (99%, Sigma-Aldrich, USA), $Gd(NO_3)_3 \cdot 6H_2O$ (99%, Sigma-Aldrich, USA), $(NH_4)_6Mo_7O_{24} \cdot 4H_2O$ (99%, Alfa Aesar, USA), $Ho(NO_3)_3 \cdot 5H_2O$ (99.9%, Sigma-Aldrich, USA), $Yb(NO_3)_3 \cdot 5H_2O$ (99.9%, Sigma-Aldrich, USA), citric acid (99.5%, Daejung Chemicals, Korea), NH_4OH (A.R.), ethylene glycol (A.R.) and distilled water were used to prepare $NaGd(MoO_4)_2$, $NaGd_{0.6}(MoO_4)_2:Ho_{0.05}Yb_{0.35}$, $NaGd_{0.55}(MoO_4)_2:Ho_{0.05}Yb_{0.40}$, $NaGd_{0.50}(MoO_4)_2:Ho_{0.05}Yb_{0.45}$ and $NaGd_{0.45}(MoO_4)_2:Ho_{0.05}Yb_{0.50}$ compounds with the correct doping concentrations of Ho^{3+} and Yb^{3+} (Ho^{3+} = 0 and 0.05, and Yb^{3+}= 0, 0.35, 0.40, 0.45 and 0.50). To prepare the compounds $Na_2MoO_4 \cdot 2H_2O$ and $(NH_4)_6Mo_7O_{24} \cdot 4H_2O$ were dissolved in 20 mL of ethylene glycol and 80 mL of 5M NH_4OH under vigorous stirring and heating. Subsequently, $Gd(NO_3)_3 \cdot 6H_2O$ with $Ho(NO_3)_3 \cdot 5H_2O$, $Yb(NO_3)_3 \cdot 5H_2O$ and citric acid (with a molar ratio of citric acid to total metal ions of 2:1) were dissolved in 100 mL of distilled water under vigorous stirring and heating. Then, the solutions were mixed together vigorously and heated at 80-100°C. Finally, highly transparent solutions were obtained and adjusted to pH=7-8 by the addition of NH_4OH or citric acid. The transparent solutions were placed into a microwave oven operating at a frequency of 2.45 GHz with a maximum output-power of 1250 W for 30 min. The working cycle of the microwave reaction was controlled very precisely using a regime of 40 s on

and 20 s off for 15 min, followed by further treatment of 30 s on and 30 s off for 15 min. The samples were treated with ultrasonic radiation for 10 min to produce a light yellowish transparent sol. After this, the light yellowish transparent sols were dried at 120°C in a dry oven to obtain black dried gels. The black dried gels were ground and heat-treated at 900°C for 16 h at 100°C intervals between 600-900°C. Finally, white particles were obtained for pure $NaGd(MoO_4)_2$ and pink particles were obtained for the doped compositions.

The phase composition of the synthesized particles was identified using XRD (D/MAX 2200, Rigaku, Japan). The microstructure and surface morphology of the synthesized particles were observed using SEM (JSM-5600, JEOL, Japan). The PL spectra were recorded using a spectrophotometer (Perkin Elmer LS55, UK) at room temperature. Pump power dependence of the UC emission intensity was measured at levels of working power from 20 to 110 mW. Raman spectra measurements were performed using a LabRam Aramis (Horiba Jobin-Yvon, France) with the spectral resolution of 2 cm^{-1}. The 514.5-nm line of an Ar ion laser was used as an excitation source; the power on the samples was kept at 0.5 mW level to avoid the sample's decomposition.

Results and discussion

Fig. 1 shows XRD patterns of the (a) JCPDS 25-0828 pattern of $NaGd(MoO_4)_2$, the synthesized (b) pure $NaGd(MoO_4)_2$, (c) $NaGd_{0.60}(MoO_4)_2$:$Ho_{0.05}Yb_{0.35}$, (d) $NaGd_{0.55}$

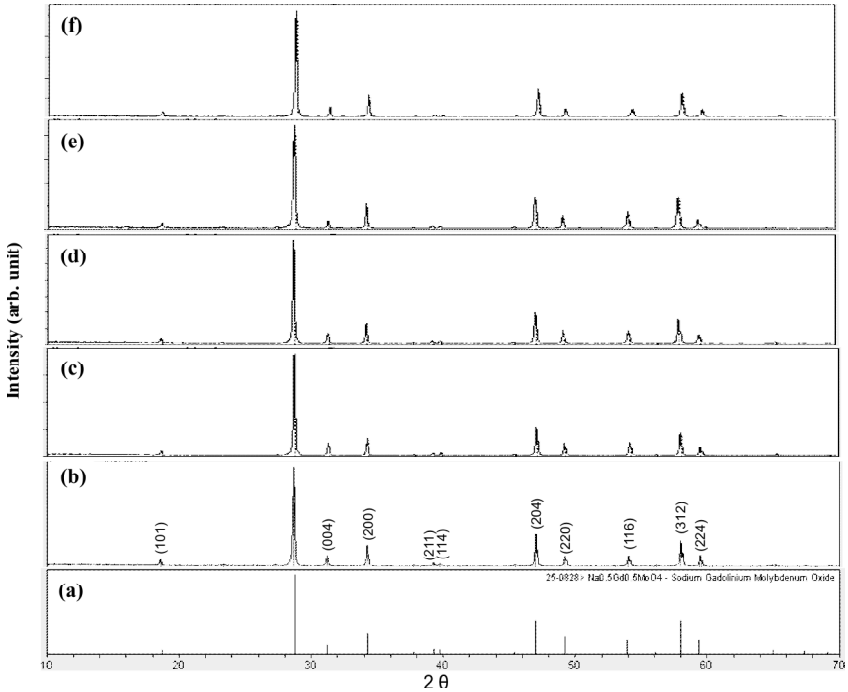

Figure 1: X-ray diffraction patterns of the (a) JCPDS 25-0828 pattern of $NaGd(MoO_4)_2$, the synthesized (b) pure $NaGd(MoO_4)_2$, (c) $NaGd_{0.60}(MoO_4)_2$:$Ho_{0.05}Yb_{0.35}$, (d) $NaGd_{0.55}(MoO_4)_2$:$Ho_{0.05}Yb_{0.40}$, (e) $NaGd_{0.50}(MoO_4)_2$: $Ho_{0.05}Yb_{0.45}$ and (f) $NaGd_{0.45}(MoO_4)_2$:$Ho_{0.05}Yb_{0.50}$ particles

$(MoO_4)_2$:$Ho_{0.05}Yb_{0.40}$, (e) $NaGd_{0.50}(MoO_4)_2$:$Ho_{0.05}Yb_{0.45}$ and (f) $NaGd_{0.45}(MoO_4)_2$: $Ho_{0.05}Yb_{0.50}$ particles. It was possible to assign almost all of the XRD peaks indexed to pure tetragonal phase, which can be mostly consistent with the standard data of $NaGd(MoO_4)_2$ (JCPDS 25-0828). $NaGd(MoO_4)_2$ as a member of double molybdate family has a sheelite structure with the lattice constants of a=5.235 Å and c=11.538 Å [15], which is tetragonal with space group $I4_{1/a}$. It can be observed, that the diffraction peaks of the doped samples of Fig. 1(c)-(f) shift slightly to the high angle compared to that of pure sample of Fig. 1(b). In the crystal structure of $NaGd_{1-x}(MoO_4)_2$, the Gd^{3+} ion site is supposed to be occupied by Ho^{3+} and Yb^{3+} ions with fixed occupations according to the nominal chemical formulas. The defined crystal structure contains MoO_4 tetrahedrons coordinated by four $(Gd/Ho/Yb)O_8$ square antiprisms through the common O ions. In the doped crystals, the unit cell shrinkage results from the substitution of Gd^{3+} ions by Ho^{3+} and Yb^{3+} ions. It is assumed that the radiuses of Ho^{3+} (R=1.015 Å) and Yb^{3+} (R=0.985 Å) are smaller than that of Gd^{3+} (R=1.053 Å), when the coordination number is CN = 8 [21]. Consequently, it should be emphasized that the Ho^{3+} and Yb^{3+} ions can be effectively doped in the $NaGd_{1-x}(MoO_4)_2$ lattice by partial substitution of Gd^{3+} site, which leads to the unit cell shrinkage due to the similar radii of Gd^{3+} and by partial substitution of Ho^{3+} and Yb^{3+} while maintaining the tetragonal structure of the $NaGd_{1-x}(MoO_4)_2$. Post heat-treatment plays an important role in a well-defined crystallized morphology. To achieve a well-defined crystalline morphology, the phases need to be heat treated at 900°C for 16 h. It is assumed that the doping concentrations of Ho^{3+}/Yb^{3+} has a suitable effect on the crystalline cell volume maintaining the original structure of the $NaGd(MoO_4)_2$.

Fig. 2 provides SEM images of the synthesized (a) $NaGd_{0.60}(MoO_4)_2$: $Ho_{0.05}Yb_{0.35}$ and (b) $NaGd_{0.45}(MoO_4)_2$: $Ho_{0.05}Yb_{0.50}$ particles. The as-synthesized samples are well crystallized with a fine and homogeneous morphology and particle size of 1-3 μm. The samples have no discrepancy in aspect of morphological feature, and agglomerated particles induced by the inter-diffusions among the grains. It should be noted that the doping concentrations for Ho^{3+} and Yb^{3+} have no effects on the morphological feature. The microwave sol-gel method of the double moybdates provides the energy to synthesize the bulk of the material uniformly, so that fine particles with controlled morphology can be fabricated in a short time period. The method is a cost-effective way to fabricate highly homogeneous products with easy scale-up and is a viable alternative for the rapid synthesis of UC particles. This suggests that the microwave sol-gel route is suitable for the creation of homogeneous $NaGd_{1-x}(MoO_4)_2$:Ho^{3+}/Yb^{3+} crystallites.

Fig. 3 shows the UC photoluminescence emission spectra of (a) $NaGd_{0.60}(MoO_4)_2$: $Ho_{0.05}Yb_{0.35}$, (b) $NaGd_{0.55}(MoO_4)_2$: $Ho_{0.05}Yb_{0.40}$, (c) $NaGd_{0.50}(MoO_4)_2$: $Ho_{0.05}Yb_{0.45}$ and (d) $NaGd_{0.45}(MoO_4)_2$: $Ho_{0.05}Yb_{0.50}$ particles excited under 980 nm at room temperature. The doped samples exhibited strong yellow emissions based on the combination of strong emission bands at 545-nm and 655-nm emission bands in green and red spectral regions, respectively. The strong 545-nm emission band in the green region corresponds to the $^5S_2/^5F_4 \rightarrow {}^5I_8$ transition in Ho^{3+} ions, while the strong 655-nm emission band in the red region appears due to the $^5F_5 \rightarrow {}^5I_8$ transition in Ho^{3+} ions. The Ho^{3+} ion activator is the

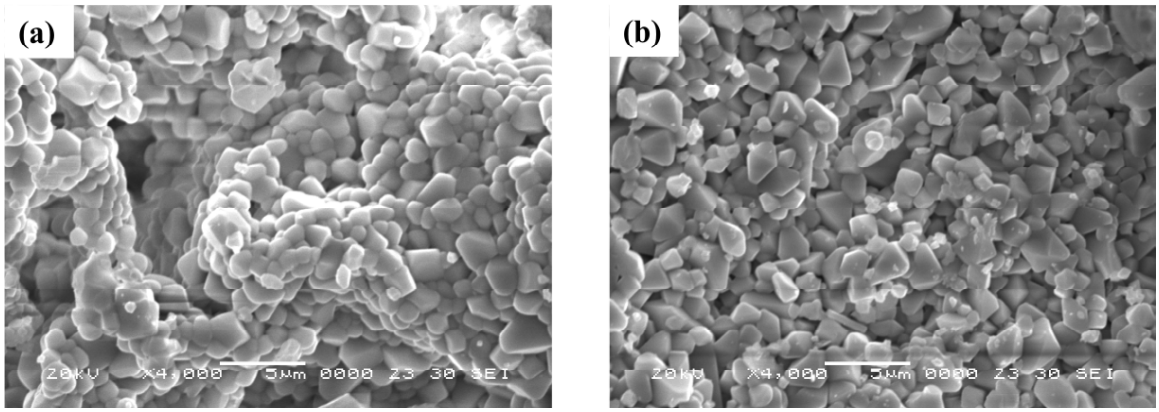

Figure 2: Scanning electron microscopy images of the synthesized (a) $NaGd_{0.60}(MoO_4)_2:Ho_{0.05}Yb_{0.35}$ and (b) $NaGd_{0.45}(MoO_4)_2:Ho_{0.05}Yb_{0.50}$ particles

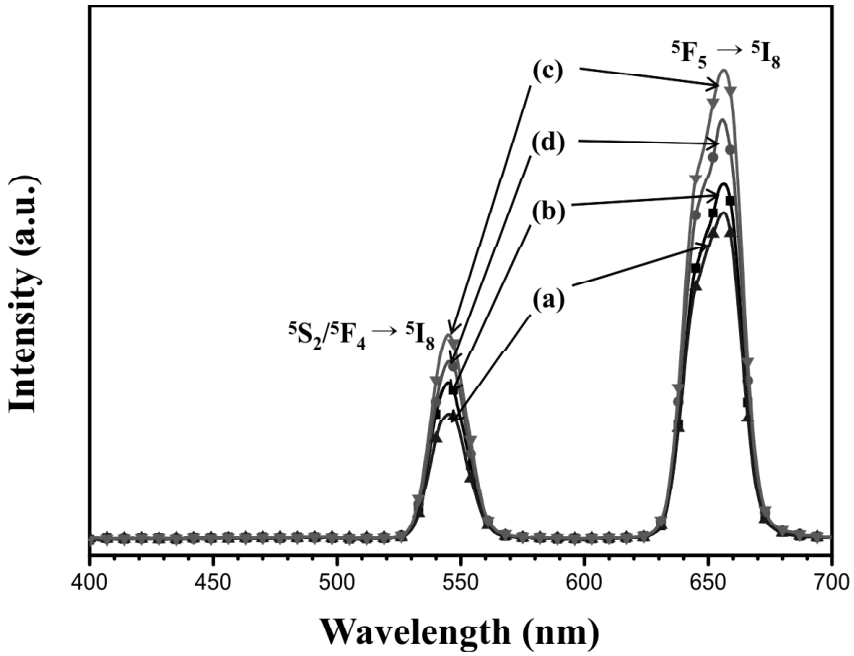

Figure 3: The upconversion photoluminescence emission spectra of (a) $NaGd_{0.60}(MoO_4)_2:Ho_{0.05}Yb_{0.35}$, (b) $NaGd_{0.55}(MoO_4)_2:Ho_{0.05}Yb_{0.40}$, (c) $NaGd_{0.50}(MoO_4)_2:Ho_{0.05}Yb_{0.45}$ and (d) $NaGd_{0.45}(MoO_4)_2:Ho_{0.05}Yb_{0.50}$ particles excited under 980 nm at room temperature

luminescence center of these UC particles, and the sensitizer Yb^{3+} effectively enhances the UC luminescence intensity because of the efficient energy transfer from Yb^{3+} to Ho^{3+}. The UC intensity is dependent on the Yb^{3+}:Ho^{3+} ratio in samples (a) 7:1, (b) 8:1, (c) 9:1 and (d) 10:1. The higher intensity of (c) $NaGd_{0.50}(MoO_4)_2$: $Ho_{0.05}Yb_{0.45}$ caused the ratio of Yb^{3+}:Ho^{3+} to be 9:1, whereas the higher contents of the Yb^{3+} ion, used as a sensitizer owing to its

strong absorption at around 980 nm, can remarkably enhance the UC luminescence through energy transfer. The concentration quenching effect can be explained by the energy transfer between nearest Ho^{3+} and Yb^{3+} ions. With increasing Ho^{3+} and Yb^{3+} ion concentrations, the distance between Ho^{3+} and Yb^{3+} ions decrease, which can promote non-radiative energy transfer such as an exchange interaction or multipole-multipole interactions [22]. The concentration quenching of upconversion emissions could be mainly attributed to the different doping ions [25]. As shown in Fig. 3, the higher intensity of (c) $NaGd_{0.50}(MoO_4)_2$: $Ho_{0.05}Yb_{0.45}$ caused the ratio of Yb^{3+}:Ho^{3+} to be 9:1, while the lower intensity of (a) $NaGd_{0.60}(MoO_4)_2$:$Ho_{0.05}Yb_{0.35}$ caused the ratio of Yb^{3+}:Ho^{3+} to be 7:1. The optimal Yb^{3+}:Ho^{3+} ratio was provided to be 9:1 induced by the concentration quenching effect of Ho^{3+} ion. Therefore, the higher content of the Yb^{3+} ion used as a sensitizer and lower content of the Ho^{3+} ion for the correct ratio of Yb^{3+}:Ho^{3+} (9:1) can remarkably enhance the UC luminescence through the efficient energy transfer.

The logarithmic scale dependence of the UC emission intensities at 545 and 655 nm on the working pump power over the range of 20 to 110 mW in the $NaGd_{0.50}(MoO_4)_2$:$Ho_{0.05}Yb_{0.45}$ sample is shown in Fig. 4. In the UC process, the UC emission intensity is proportional to the slope value n of the irradiation pumping power, where n is the number of pumped photons required to produce UC emission [23]:

$$I \propto P^n \tag{1}$$

$$\mathrm{Ln}I \propto n\mathrm{Ln}P \tag{2}$$

Where value n is the number of the pumped photons required to excite the upper emitting state, I is the UC luminescent intensity and P is the laser pumping power. The calculated slope values n in Fig. 4 indicate slope n = 1.85 for green emission at 545 nm; this value is 1.96 for red emission at 655 nm. These results show that the UC mechanism of the green and red emissions can be explained by a two-photon UC process in Er^{+3}/Yb^{3+} co-doped phosphors [24, 25] as well as in Ho^{+3}/Yb^{3+} co-doped phosphors [4, 12].

Fig. 5 shows the Raman spectra of the synthesized (a) pure $NaGd(MoO_4)_2$, (b) $NaGd_{0.60}(MoO_4)_2$: $Ho_{0.05}Yb_{0.35}$, (c) $NaGd_{0.55}(MoO_4)_2$:$Ho_{0.05}Yb_{0.40}$, (d) $NaGd_{0.50}(MoO_4)_2$:$Ho_{0.05}Yb_{0.45}$ and (e) $NaGd_{0.45}(MoO_4)_2$:$Ho_{0.05}Yb_{0.50}$ particles excited by the 514.5-nm line of an Ar ion laser at 0.5 mW. The internal modes for the (a) pure $NaGd(MoO_4)_2$ particles were detected at 330, 384, 818, 892, 994 and 1333 cm^{-1}, respectively. The well-resolved sharp peaks for the $NaGd(MoO_4)_2$ indicate a high crystallinity state of the synthesized particles. The internal vibration mode frequencies are dependent on the lattice parameters and the strength of the partially covalent bond between the cation and molecular ionic group MoO_4. The Raman spectrum of the $NaGd(MoO_4)_2$ crystal in Fig. 7(a) shows the typical molybdate compounds, which is divided into two parts with a wide empty gap of 400-800 cm^{-1}. The highest intensity of the wavenumber band at 892 cm^{-1} corresponds to stretching vibrations of the MoO_4. The stretching vibrations of Mo-O bonds are observed at 818 cm^{-1} regions. For these stretching vibrations, strong mixing occurs between the Mo-O bonds and the MoO_4. The band at 323 and 394 cm^{-1} could be assumed to originate from vibrations of the longer Mo-O bonds, which are employed in the formation of the Mo-Mo bridge. The

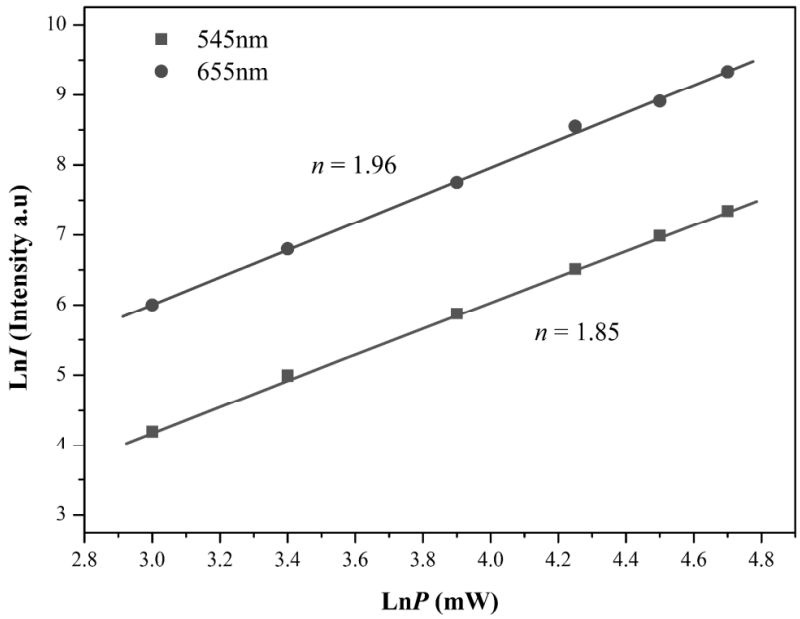

Figure 4: Logarithmic scale dependence of the upconversion emission intensity on the pump power in the range from 20 to 110 mW at 545 and 655 nm in the $NaGd_{0.50}(MoO_4)_2:Ho_{0.05}Yb_{0.45}$ sample

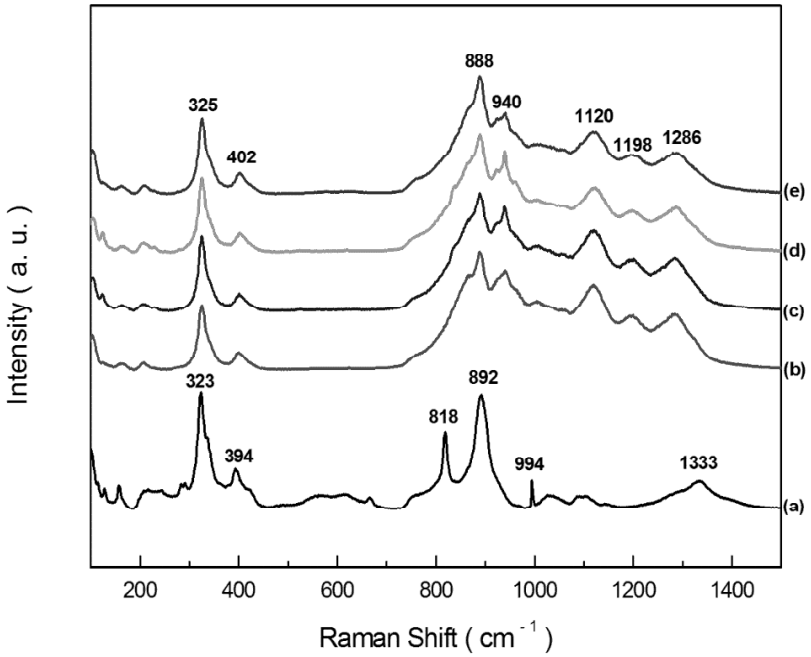

Figure 5: Raman spectra of the synthesized (a) pure $NaGd_2(MoO_4)_4$, (b) $NaGd_{0.60}(MoO_4)_2:Ho_{0.05}Yb_{0.35}$, (c) $NaGd_{0.55}(MoO_4)_2:Ho_{0.05}Yb_{0.40}$, (d) $NaGd_{0.50}(MoO_4)_2$: $Ho_{0.05}Yb_{0.45}$ and (e) $NaGd_{0.45}(MoO_4)_2:Ho_{0.05}Yb_{0.50}$ particles excited by the 514.5-nm line of an Ar ion laser at 0.5 mW

Raman spectra of (b) $NaGd_{0.60}(MoO_4)_2:Ho_{0.05}Yb_{0.35}$, (c) $NaGd_{0.55}(MoO_4)_2:Ho_{0.05}Yb_{0.40}$, (d) $NaGd_{0.50}(MoO_4)_2:Ho_{0.05}Yb_{0.45}$ and (e) $NaGd_{0.45}(MoO_4)_2:Ho_{0.05}Yb_{0.50}$ particles indicate the very strong and dominant peaks at higher frequencies of 888, 940, 1120, 1198 and 1286 cm^{-1} and at lower frequencies of 326 and 402 cm^{-1}. These strong disordered peaks at higher frequencies are attributed to the formation of modulated structures of $NaGd_{1-x}(MoO_4)_2$ due to the strong mixing between the Mo-O bonds and the MoO_4 stretching vibrations by the incorporation of the Ho^{3+} and Yb^{3+} elements into the crystal lattice, which result in the unit cell shrinkage that accompanies the highly modulated MoO_{4-x} group. These incommensurately modulated structures were also observed in several molybdate and tungstate compounds [25-27]. Previously, our research group has reported on this strongly dominant spectra of the incommensurately modulated structure in the case of $CaGd_2(WO_4)_4:Er^{3+}/Yb^{3+}$ phosphors [28]. It should be emphasized that the strongly dominant spectra are attributed to the strong mixing between the Mo-O bonds and the MoO_4 stretching vibrations as well as the concentration quenching effect of Ho^{3+} ions. These results lead to high emitting efficiency and superior thermal and chemical stability, and these materials, which can overcome the current limitations of traditional photoluminescence materials, can be considered potentially active components in new optoelectronic devices and in luminescent imaging.

Conclusions

$NaGd_{1-x}(MoO_4)_2:Ho^{3+}/Yb^{3+}$ UC phosphors with the correct doping concentrations of Ho^{3+} and Yb^{3+} were successfully synthesized via the microwave sol-gel route. Well-crystallized particles formed after heat-treatment at 900°C for 16 h showed a fine and homogeneous morphology with particle sizes of 1-3 μm. Under excitation at 980 nm, the UC doped particles exhibited yellow emissions based on a strong 545-nm emission band in the green region and a very strong 655-nm emission band in the red region, which were assigned to the $^5S_2/^5F_4 \rightarrow {}^5I_8$ and $^5F_5 \rightarrow {}^5I_8$ transitions, respectively. The higher intensity of $NaGd_{0.50}(MoO_4)_2:Ho_{0.05}Yb_{0.45}$ provided that the ratio of Yb^{3+}:Ho^{3+} would be 9:1, whereas the higher contents of Yb^{3+} ion as a sensitizer owing to its strong absorption around 980 nm can remarkably enhance the UC luminescence through energy transfer. The calculated slope values *n* indicate slope $n = 1.85$ for green emission at 545 nm; this value is 1.96 for red emission at 655 nm. This result indicates the achievement of attractive yellow UC emissions for use potentially active components in new optoelectronic devices and luminescent devices.

Acknowledgement

This research was supported by the Basic Science Research Program through the National Research Foundation of Korea (NRF) funded by the Ministry of Education (2016-944122).

References

[1] M. Wang, G. Abbineni, A. Clevenger, C. Mao, S. Xu, Nanomedicine: Nanotech. Biology, and Medicine, 7, 710 (2011).

[1] M.V. DaCosta, S. Doughan, U.J. Krull, Analyca Chimica Acta, 832, 1 (2014).

[2] M. Lin, Y. Zho, S. Wang, M, Liu, Z. Duan, Y. Chen, F. Li, F. Xu, T. Lu, Biotechnol. Adv., 30, 1551 (2012).

[3] M. Wang, G. Abbineni, A. Clevenger, C. Mao, S. Xu, Nanomed.: Nanotech. Biol. Med., 7, 710 (2011).

[4] C.S. Lim, A. Aleksandrovsky, M. Molokeev, A. Oreshonkov, V. Atuchin, Phys. Chem. Chem. Phys., 17, 19278 (2015).

[5] C.S. Lim, Mater. Res. Bull., 75, 211 (2016).

[6] L. Li, W. Zi, H. Yu, S. Gan, G. Ji, H. Zou, X. Xu, J. Lumin., 143, 14 (2013).

[7] C. Ming, F. Song, L. Yan, Opt. Commun., 286, 217 (2013).

[8] N. Xue, X. Fan, Z. Wang, M. Wang, J. Phys. Chem. Sol., 69, 1891 (2008).

[9] Z. Shan, D. Chen, Y. Yu, P. Huang, F. Weng, H. Lin, Y. Wang, Mater. Res. Bull., 45, 1017 (2010).

[10] W. Liu, J. Sun, X. Li, J. Zhang, Y. Tian, S. Fu, H. Zhong, T. Liu, L. Cheng, H. Xia, B. Dong, R. Hua, X. Zhang, B. Chen, Opt. Mater., 35, 1487 (2013).

[11] W. Xu, H. Zhao, Y. Li, L. Zheng, Z. Zhang, W. Cao, Sensors and Act. B:Chem., 188, 1096 (2013).

[12] J. Tang, C. Cheng, Y. Chen, Y. Huang, J. Alloys Compd., 609, 268 (2014).

[13] J. Liao, H. Huang, H. You, X. Qiu, Y. Li, B. Qui, H-R Wen, Mater. Res. Bull., 45, 1145 (2010).

[14] G.M. Kuz'micheva, D.A. Lis, K.A. Subbotin, V.B. Rybakov, E.V. Zharikov, J. Crys. Growth, 275, e1835 (2005).

[15] H. Lin, X. Yan, X. Wang, J. Sol. State. Chem., 204, 266 (2013).

[16] J. Zhang, X. Wang, X. Zhang, X. Zhao, X. Liu, L. Peng, Inorg. Chem. Commun., 14, 1723 (2011).

[17] S.W. Park, B.K. Moon, B.C. Choi, J.H. Jeong, J.S. Bae, K.H. Kim, Curr. Appl. Phys., 12, S150 (2012).

[18] C.S. Lim, Mater. Res. Bull., 47, 4220 (2012).

[19] C.S. Lim, Mater. Chem. Phys., 131, 714 (2012).

[20] C.S. Lim, Infrar. Phys. Tech., 67, 371 (2014).

[21] R. D. Shanan, Acta Cryst., A32, 751 (1976).

[22] F. Anzel, G. Baldacchini, L. Laversenne, G. Boulon, Opt. Mat., 24, 103 (2003).

[23] H. Guo, N. Dong, M. Yin, W. Zhang, L. Lou, S. Xia, J. Phys. Chem. B, 108, 19205 (2004).

[24] H. Du, Y. Lan, Z. Xia, J. Sun, Mater Res. Bull., 44, 1660 (2009).

[25] A.M. Abakumov, V.A. Morozov, A.A. Tsirlin, J. Verbeeck, J. Hadermann, Inorg. Chem., 53, 9407 (2014).

[26] V.A. Morozov, A. Bertha, K.W. Meert, S. Van Rompaey, D. Batuk, G.T. Martinez, S. Van Aert, P.F. Smet, M.V. Raskina, D. Poelman, A.M. Abakumov, J. Hadermann, Chem. Mat., 25, 4387 (2013).

[27] V. A. Morozov, A.V. Mironov, B.I. Lazoryak. E.G. Khaikina, O.M. Basovich, M.D. Rossell, G.V. Tendeloo, J. Solid State Chem., 179, 1183 (2006).

[28] C.S. Lim, A. Aleksandrovsky, M. Molokeev, A. Oreshonkov, V. Atuchin, J. Solid State Chem., 228, 160 (2015).